MODELING THE ACTION OF SECONDARY FLOWS ON THE MIXING PROCESS IN A CHANNEL

V. I. Vasil'ev and S. N. Zakotenko

UDC 532.522.2:519.63

1. In order to intensify the mixing of two flows in a channel, in a number of cases lobe-shaped profiled nozzles of the type shown in Fig. 1 may be installed in front of the common chamber. These nozzles have a developed exit perimeter and therefore increase the overall intensity of turbulent transfer. Moreover, passage over the profiled surface may lead to the formation of strong secondary flows, which also promote mixing.

In [1, 2] a method of calculating flow mixing in the presence of intense cross flows, based on the numerical integration of parabolic equations is proposed. Accordingly, the cross flows in the chamber inlet section must be given. In [2] the experimental results of [3] were used for this purpose. In the same study a simplified method of modeling secondary flows is proposed. The auxiliary problem of three-dimensional ideal-gas flow past a nozzle with a tangential discontinuity behind the edge is therefore solved and the transverse velocity field in the exit section is found. In view of the fact that in mixers with lobe-shaped nozzles the Mach numbers are usually small (≤ 0.5), it is permissible to solve the problem in the incompressible approximation.

2. We will consider the auxiliary problem for an annular channel (or a channel of rectangular cross section) with cylindrical inlet and outlet (Fig. 1, the contour is shown as a continuous line). In modeling the real mixer (broken line) it may be assumed that the inlet and outlet sections are abutted by cylindrical parts of infinite extent. The surface separating the two flows at the inlet is a circular cylindrical surface (or plane), and its profiled part can be described by relations of the form:

$$y = Y(x, t),\ z = Z(x, t), \tag{2.1}$$

where x, y, and z are Cartesian coordinates, t is a parameter (for example, polar angle in the yz plane), and the functions Y, Z are periodic in t. Behind the rear edge of the separator a surface of tangential discontinuity, assumed to belong to the class of surfaces of the form (2.1), is introduced. The rear edge of the separator lies either in the section $x = \text{const}$ (normal cutoff) or (oblique cutoff) on the conical surface $\alpha(y^2 + z^2) = (\text{const} - x)^2$ (for a rectangular channel, in the plane, $x + \alpha y = \text{const}$).

In what follows the parameters below the separator are identified by the subscript 1, those above the separator by the subscript 2. The flow in channels 1 and 2 is assumed to be potential. Since the inlet and outlet are cylindrical, the inlet ($x \to -\infty$) and outlet ($x \to +\infty$) flows are uniform, and as $x \to +\infty$ the surface of tangential discontinuity asymptotically approaches the cylindrical. The boundary value problems for determining the velocity potentials φ in channels 1 and 2 can be formulated as follows:

$$\frac{\partial^2 \varphi_i}{\partial x^2} + \frac{\partial^2 \varphi_i}{\partial y^2} + \frac{\partial^2 \varphi_i}{\partial z^2} = 0, \quad i = 1, 2; \tag{2.2}$$

$$x = x_0,\ \frac{\partial \varphi_i}{\partial x} = -U_i;\ x = x_e;\ \varphi_i = 0,\ \mathbf{r} \in S,\ \frac{\partial \varphi_i}{\partial n} = 0,\ i = 1, 2. \tag{2.3}$$

Here, $\partial/\partial n$ is the derivative with respect to the normal to the flow surface, r is the radius vector of the point, U is the velocity of the uniform flow at the inlet. The velocity vector V with components V_x, V_y, V_z is equal to the gradient of φ with the opposite sign ($\mathbf{V} = -\nabla\varphi$), V is the modulus of the velocity. Generally speaking the first two conditions (2.3) must be carried to infinity, i.e., $x_0 \to -\infty$, $x_e \to +\infty$. However, in the numerical solution of the problem it is necessary to consider a finite domain, and choose the parameters x_0 and x_e so that

Moscow. Translated from Zhurnal Prikladnoi Mekhaniki i Tekhnicheskoi Fiziki, No. 3, pp. 156-161, May-June, 1991. Original article submitted August 7, 1989; revision submitted November 28, 1989.

0021-8944/91/3203-0449$12.50

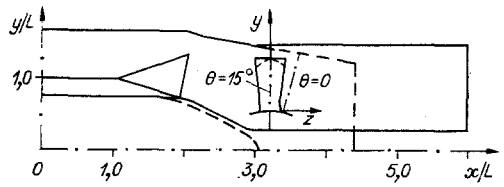

Fig. 1

the solution does not depend on their value. In order to determine the shape of the surface of tangential discontinuity it is necessary to use the condition of continuity of the static pressure. By means of the Bernoulli integral this condition can be reduced to

$$V_1^2 - V_2^2 = D_p. \tag{2.4}$$

The constant D_p is not known in advance, since the problem with given flowrates is considered, and the total pressure difference, proportional to the left side of (2.4), must be determined. The parameter D_p can be found by requiring the satisfaction of the condition of finiteness of the velocity at the rear edge (Chaplygin–Joukowski postulate).

In general, an explicit functional dependence of the velocity distribution on the parameters determining the shape of the tangential discontinuity is not known. Therefore it is not possible to invert the relation (2.4) and the surface of tangential discontinuity is found by means of iterations, which are so carried out that, finally, the no-slip conditions [last condition in (2.3)] and relation (2.4) on the discontinuity are satisfied. As the initial approximation we take the surface that smoothly joins the surface of the separator at the rear edge, i.e., the common flow surface of channels 1 and 2 is a Lyapunov surface. Boundary value problems (2.2) and (2.3) are solved, and as a result we find the potential and velocity distributions on the surface. We then recalculate the coordinates of points on the surface of discontinuity in accordance with the expression

$$\Delta \mathbf{r}(x, t) = \left(\left[V_c^2(t)\right] - \left[V^2(x, t)\right]\right) \cdot \mathbf{n} \cdot \gamma, \tag{2.5}$$

where $\Delta \mathbf{r}$ is the increment of the coordinates of a point on the surface described by relations (2.1), $\mathbf{n}$ is the outward normal with respect to flow 1, the square brackets denote the difference between the parameters of flows 1 and 2, γ is an iteration parameter, and V_c is the distribution of the velocity modulus along the edge. As soon as the new position of the surface of discontinuity has been found, the entire procedure is repeated, and so on to convergence. For solving boundary value problems (2.2), (2.3) we used the boundary-integral equation method [4].

3. In order to test the iteration method we considered two model problems. In the first we calculated the flow in a plane channel of constant width H with a separator whose surface was composed of segments of planes: $y/L = 1$ when $x \leq -1$, $y - \tan\alpha \cdot x = 0$ when $-1 \leq x \leq 0$. As the characteristic length L we chose the projection of the deflected tail of the separator on the x axis, $H/L = 2$, and the lower wall is located at $y = 0$, $\alpha = 15°$. For this channel it is possible to find a particular analytic solution. In fact, by means of the Schwarz–Christoffel integral the flow domain in the plane $\eta = x + iy$ can be mapped onto the upper half-plane of the auxiliary complex variable ξ:

$$\eta - \eta_c = \frac{2}{\pi} \int_c^{\xi} \left(\frac{\tau - b}{\tau - a}\right)^{\alpha/\pi} \left(\frac{\tau - c}{\tau^2 - 1}\right) d\tau \tag{3.1}$$

(η_c is the coordinate of the point on the rear edge). The transformation parameters can be found from the relations

$$\left(\frac{1-b}{1-a}\right)^{\alpha/\pi}(1-c) = 1, \quad \left(\frac{1+b}{1+a}\right)^{\alpha/\pi}(1+c) = 1, \quad \int_0^b \left(\frac{b-\tau}{\tau-a}\right)^{\alpha/\pi} \left(\frac{\tau-c}{1-\tau^2}\right) d\tau = \frac{\pi}{2}, \tag{3.2}$$

where $-1 < a < c < 0 < b < 1$. Assuming the angle α to be small, from this we obtain $b = -a = \sqrt{1 - \exp(-\pi)} + O(\alpha)$, $c = -(\alpha/\pi)\ln((1 + b)/(1 - b)) + O(\alpha^2)$. The accuracy can subsequently

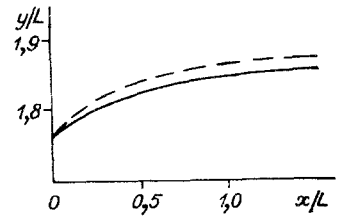

Fig. 2

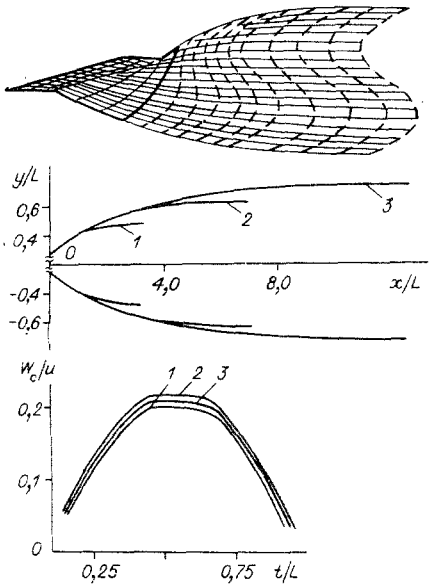

Fig. 3

be improved numerically by means of relations (3.2). We note that here the integral is non-singular.

The complex potential of the continuous flow in the channel in the upper half-plane of ξ is two-source flow potential:

$$\chi = \varphi + i\psi = \frac{U_1}{\pi}\left[\ln(\xi - 1) + \frac{1+c}{1-c}\ln(\xi + 1)\right] \tag{3.3}$$

(ψ is the stream function). The solution (3.3) satisfies the Chaplygin–Joukowski postulate and is a particular case describing the flow in a channel with a separator when $D_p = 0$ (for the indicated values of the geometric parameters this corresponds to the condition $U_2/U_1 = 0.46$). Having calculated the root of the equation $\mathrm{Im}\,\chi = U_1$, we obtain the image of the streamline departing from the rear edge, and after evaluating the integral (3.1) we can determine its position in the physical plane.

In Fig. 2 the solution in question (continuous curve) is compared with the numerical calculations (broken curve). Despite the fact that the numerical calculations were carried out on a rather coarse grid, with the separatrix divided into only five parts, the agreement between the numerical and exact solutions is perfectly satisfactory, the error in determining the separatrix being 2% and the error in determining the velocity fields of the order of 3%.

In the second example we introduced into the same channel a separator whose surface is described by the relations

$$\frac{y}{L} = 0 \text{ when } \frac{x}{L} \leqslant -1, \quad \frac{y}{L} = \left(\frac{x}{L}\right)\mathrm{tg}\,(15^\circ)\cos\left(\pi\frac{z}{0{,}75L}\right) \text{ when } -1 \leqslant \frac{x}{L} \leqslant 0,$$

in this case $0 \leq z/L \leq 0.75$. The flow in this channel is essentially three-dimensional and periodic in z with period equal to 1.5. We investigated the case $U_2/U_1 = 1$, which in the situation in question corresponds to $D_p = 0$.

Figure 3 shows the general appearance of the surface of the separator and the tangential discontinuity (top); the diagram corresponds to a half-period with respect to z. It is interesting to note that the surface of the separator is described by a function of the form $y = Y(x, z)$, but the surface of discontinuity belongs to the more general class (2.1), where the line of intersection of this surface with the yz plane is a parametric curve.

With reference to this example we investigated the effect of the position of the inlet and outlet boundaries of the computation domain on the result. If the length of the cylin-

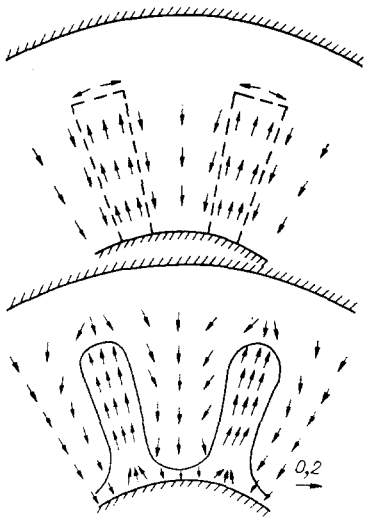

Fig. 4

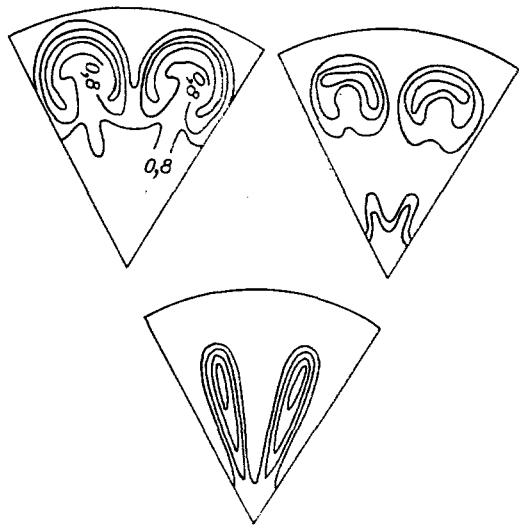

Fig. 5

drical inlet sections $\Delta x/L > 1$, the result is almost independent of the value of x_0. The position of the outlet boundary has a more important effect. In the middle of Fig. 3 we have plotted the lines of intersection of the surface of discontinuity with the planes z = 0 and z/L = 0.75, obtained for different positions of the outlet boundary (curves 1-3 correspond to x_e/L = 5.3, 9.3, and 14.6). Clearly, the asymptote is approached slowly, and to obtain the asymptotic position of the end of the surface of discontinuity it is necessary to take $x_e/L \geq 15.0$. However, both the shape of the surface near the edge and the transverse velocity distribution in the separator cutoff section are quite weakly sensitive to the position of the outlet section. This situation is illustrated by the transverse velocity distribution $W_c = \sqrt{V_y^2 + V_z^2}$ along the edge of the separator in the section x = 0 obtained for three values of x_e/L (bottom of Fig. 3). As x_e increases convergence is observed, and for determining the cross flows with an acceptable relative error of 5% it is possible to locate the outlet section at $x_e/L \sim 5.0$, and thereby avoid excessive computation.

4. In order to study the possibilities of modeling the action of secondary flows on the mixing process we examined the flow in the mixer shown in Fig. 1 (broken contour). This flow was calculated in [2], where the values of all the parameters determining the flow regime were also given. In [2] the velocity field in projection on the nozzle exit surface $\mathbf{W}_c$ was taken from the experiments reported in [3]. In the present study we repeated the calculations using the method of [2], but found $\mathbf{W}_c$ from the solution of the auxiliary problem.

To the real mixer we fitted cylindrical inlet and outlet sections (continuous line in Fig. 1), whose length was chosen on the basis of the results of a systematic investigation. Certain unimportant details of the petal shape, the rounding of the corners, etc., were not reproduced in the calculations (see Fig. 1). The parameter U_2/U_1 was assumed to be equal to 0.62, which corresponds to a velocity ratio of 0.86 at the inlet to the common chamber. The calculated distribution $\mathbf{W}_c/u$ (u is the velocity component along the normal to the exit surface) is similar to that obtained experimentally, as evidenced by the comparison in Fig. 4, where the calculation results are shown at the top and the experimental results at the bottom.

The results of calculating the stagnation temperature isolines at the mixer chamber outlet with the initial conditions for the cross flows determined as described above are presented in Fig. 5 (top left). The figure also shows (top right) the experimental data and, at the bottom, the results of the calculations made without taking cross flows into account. Clearly, if the cross flows are not taken into account, then the calculations are not in qualitative agreement with experiment. When the cross flows are taken into account, there is qualitative and satisfactory quantitative agreement, as in [2].

Thus, for modeling the secondary flows behind lobe-shaped nozzles at the inlet to a mixing chamber it is permissible to use the model of potential flow with a tangential discontinuity.

LITERATURE CITED

1. V. I. Vasil'ev and S. Yu. Krasheninnikov, "Calculation of three-dimensional weakly expanding flow in a jet and channel," Izv. Akad. Nauk SSSR, Mekh. Zhidk. Gaza, No. 4 (1984).
2. V. I. Vasil'ev, "Calculation of three-dimensional nozzle flow with mixing in the presence of an important vorticity effect," Inzh.-fiz. Zh., 54, No. 4 (1988).
3. B. Anderson, L. Povinelli, and W. Gerstenmaier, "Influence of pressure-driven secondary flows on the behavior of turbofan forced mixers," AIAA Paper No. 1198, New York (1980).
4. T. A. Cruse and F. J. Rizzo (eds.), Boundary-Integral Equation Method, ASME (1975).

MÖSSBAUER STUDIES OF UNIAXIALLY LOADED FERROMAGNETIC SAMPLES

V. P. Larionov and Ya. S. Semenov

UDC 539.56

Practically all constructions and materials are structurally inhomogeneous. In some cases this inhomogeneity is attributable to the material production technology, and in others it is caused by the introduction of a second phase for the purpose of investing the material with new properties. Regardless of the properties of the material, these inhomogeneities become stress concentrators, which have a powerful influence on the ductile–brittle transition temperature. The ductile–brittle transition always shifts toward positive temperatures when materials with stress concentrators are subjected to various kinds of loading [1, 2].

We have therefore undertaken a study of uniaxially stressed samples, using Mössbauer spectroscopy. We chose ferromagnetic materials whose spectra had a well-resolved Zeeman sextet. Electric quadrupole and magnetic dipole hyperfine interactions, magnetic texture modifications, relaxation phenomena [3], and hence variations of the electronic structure in uniaxial loading are easily resolved in such spectra.

EXPERIMENTAL PROCEDURE AND RESULTS

A special test stand consisting of a movable clamp and a fixed clamp was developed for the Mössbauer investigation of uniaxially loaded samples. The movable clamp is connected to the loading machine, which sets the value of the applied load.

The samples were prepared from alloys of the binary system Fe–Si with the following compositions: Fe–0.2%Si; Fe–1.0%Si; Fe–2.0%Si; Fe–3.6%Si. Foil samples were made by the standard technique in the form of ribbons of length 20-30 mm, width 20-25 mm, and thickness ~60 μm. A constant-acceleration electrodynamic spectrometer was used to obtain the Mössbauer spectra.

Figure 1 shows the Mössbauer spectra of different compositions of the binary system Fe–Si (the channel number is plotted along the horizontal axis, and the relative intensity along the vertical). Figure 1a gives the spectra of samples loaded uniaxially in the elastic domain with mass fractions of silicon equal to 2% (spectra 1-3 for σ = 0, 0.4, 6 kg/mm^2) and 3.6% (spectra 5-7 for the same values of σ). A characteristic feature is the fact that the usual Zeeman sextets for the given composition under loading exhibit an increase in the effective magnetic field, a change in the intensity ratio, and a positive isomer shift.

Figure 1b gives the Mössbauer spectra of samples with mass fractions of silicon equal to 0.2% (spectra 1-3 for σ = 0, 14, 28 kg/mm^2), 1% (spectra 4-6 for the same values of σ), and 3.6% (spectra 7 and 8 for σ = 0 kg/mm^2 and 14 kg/mm^2). These spectra exhibit changes in the intensity ratio and isomer shifts without any significant changes in the effective magnetic field as the loads are increased.

We calculated the Mössbauer spectra according to the model postulated in [4]. The results of processing of the spectra by this procedure are shown in Fig. 2, where ΔE_Q is the

Yakutsk. Translated from Zhurnal Prikladnoi Mekhaniki i Tekhnicheskoi Fiziki, No. 3, pp. 161-164, May-June, 1991. Original article submitted January 11, 1989; revision submitted December 7, 1989.

0021-8944/91/3203-0453$12.50